doi: 10.4149/gpb_2025024

circ_0049271 downregulation ameliorates lipopolysaccharide-induced human renal tubular endothelial cell apoptosis, inflammation and oxidative stress

Xiaozhen Ji[1,*], Jinjuan Zhang[2,*] and Lefeng Zhang[3,4]

[1] *Department of Emergency, Longquan People's Hospital, Longquan, China*
[2] *Science and Education Section, Longquan People's Hospital, Longquan, China*
[3] *Department of Respiratory and Critical Care Medicine, Lishui Second People's Hospital, Lishui, China*
[4] *Graduate School, Zhejiang Chinese Medical University, Hangzhou, China*

Abstract. Circular RNA (circRNA) has been confirmed to be a regulator for septic acute kidney injury (AKI). It is reported that circ_0049271 has abnormal expression in AKI patients, but its role and mechanism in septic AKI remain unclear. Lipopolysaccharide (LPS)-stimulated HK-2 cells were served as the cellular model of sepsis-associated AKI (SAKI). qRT-PCR was conducted for examining the expression of circ_0049271, KEAP1 and miR-331-3p. Cell proliferation and apoptosis were detected by EdU assay and flow cytometry. The protein levels of apoptosis-related markers, RUNX family transcription factor 1 (RUNX1), and PI3K/AKT/mTOR pathway-related markers were tested using Western blot. RNA interaction was confirmed by dual-luciferase reporter assay, RIP assay, and RNA pull-down assay. Our data showed that circ_0049271 was enhanced in LPS-induced HK-2 cells. Silencing of circ_0049271 attenuated LPS-induced HK-2 cell oxidative stress, apoptosis, and inflammation. In terms of mechanism, circ_0049271 targeted miR-331-3p to promote LPS-induced HK-2 cell injury. RUNX1 was a target of miR-331-3p, and RUNX1 overexpression reversed miR-331-3p-mediated inhibitory effects on LPS-induced HK-2 cell injury. Moreover, circ_0049271 sponged miR-331-3p to positively regulate RUNX1 expression, thus activating the PI3K/AKT/mTOR pathway. In conclusion, our data indicated that circ_0049271 contributed to LPS-induced HK-2 cell injury by regulating miR-331-3p/RUNX1 pathway, providing potential molecular targets for the treatment of SAKI.

Key words: Sepsis — SAKI — circ_0049271 — miR-331-3p — RUNX1

Introduction

Sepsis is a syndrome with systemic inflammatory response to severe infection (Fleischmann-Struzek et al. 2020; Font et al. 2020; Nedeva 2021). Acute kidney injury (AKI) is one of the most frequent organ dysfunction in the process of sepsis (Manrique-Caballero et al. 2021). Despite the improved therapy, sepsis-associated AKI (SAKI) contributes to high mortality in sepsis patients (Poston and Koyner 2019). Renal tubular epithelial cells (RTECs) are the major cell type in kidney tissues and work as the crucial etiologic effector of SAKI (An et al. 2023). The pathophysiology of SAKI involves several pathophysiological processes including RTECs apoptosis, oxidative stress, and inflammatory response (Li et al. 2023). At present, human renal tubular epithelial cells (HK-2) stimulated by lipopolysaccharide (LPS) have been used as *in vitro* cell models for studying the molecular mechanisms of SAKI (Kim et al. 2021; Stasi et al. 2021; Sun et al. 2021).

* These authors contributed equally to this study.
Correspondence to: Lefeng Zhang, Graduate School, Zhejiang Chinese Medical University, No. 548 Binwen Road, Binjiang District, Hangzhou, 310056, China
E-mail: lefeng_zhangg@163.com; 2001090610@alu.zcmu.edu.cn

© The Authors 2025. This is an **open access** article under the terms of the Creative Commons Attribution-NonCommercial 4.0 International License (https://creativecommons.org/licenses/by-nc/4.0/), which permits non-commercial use, distribution, and reproduction in any medium, provided the original work is properly cited.

Circular RNAs (circRNAs) are featured with stable closed-loop structures (Kristensen et al. 2019). Various studies have proved that circRNAs can serve as crucial regulators in multiple diseases (Verduci et al. 2021), including sepsis (Beltran-Garcia et al. 2020). circRNAs can act as competing endogenous RNAs (ceRNAs) to regulate sepsis *via* sponging miRNA (Qi et al. 2021). For instance, circTLK1 knock-down inhibited cell injury in LPS-induced HK-2 cell *in vitro* model *via* regulating miR-106a-5p/HMGB1 axis (Xu et al. 2021). For another example, circTtc3 promoted inflammatory response and oxidative stress in SAKI rat model through miR-148a/Rcan2 (Ma et al. 2021). A previous circRNA microarray analysis demonstrated that circ_0049271 was elevated in serum exosomes of SAKI patients (Tian C et al. 2021). Therefore, circ_0049271 has the potential to be a molecular target for SAKI treatment. However, the roles and mechanisms of circ_0049271 in SAKI progression remain to be investigated.

MicroRNAs (miRNAs) are short (~22 nucleotides) RNAs and have been proved to function in multiple human diseases (Gebert and MacRae 2019). Also, miRNAs serve as important regulators in SAKI (Ma J et al. 2019; Ma P et al. 2020). A previous study showed that miR-331-3p was lowly expressed in sepsis patients, and its over-expression alleviated vascular endothelial cell injury by inhibiting CLDN2 expression (Kong et al. 2020). RUNX family transcription factor 1 (RUNX1) has been confirmed to be upregulated in renal tissues of SAKI rat models, and its knockdown improved renal function (Zhang Y et al. 2021). Also, circ_0049271 was found to have binding sites with miR-331-3p, and miR-331-3p could bind to RUNX1 3'UTR. However, whether circ_0049271 regulates miR-331-3p/RUNX1 axis to mediate SAKI progression remains unclear.

Here, we assessed the regulatory function and mechanism of circ_0049271 in a LPS-stimulated HK-2 cell model. The proposed circ_0049271/miR-331-3p/RUNX1 axis may provide potential target for SAKI treatment.

Materials and Methods

Cell culture and treatment

HK-2 cell (Procell, Wuhan, China) was cultured in MEM containing 10% FBS and 1% penicillin/streptomycin. LPS is a commonly used inflammatory agent that can be used to induce HK-2 cell inflammation models to study the mechanism of SAKI (Yang et al. 2024; Zhang et al. 2024). To simulate the sepsis *in vitro*, different concentration of LPS (0, 2.5, 5, 10, 20 μg/ml; Solarbio, Beijing, China) was used to treat HK-2 cells for 24 h to choose a proper stimulatory concentration.

qRT-PCR

TRIzol reagent (Invitrogen, Carlsbad, CA, USA) was adopted to isolate total RNA. Then, the reverse transcription was conducted by PrimeScript RT Master Mix Kit (TaKaRa, Dalian, China). Next, SYBR Premix Ex Taq II (TaKaRa) was mixed with cDNA together with specific primers (Table 1) for qRT-PCR. Relative levels were calculated by the $2^{-\Delta\Delta Ct}$ method.

RNase R and actinomycin D (Act D) treatment

Total RNA was treated with or without RNase R (Seebio, Shanghai, China) for 30 min, followed by RNA extraction and qRT-PCR to detect the levels of circ_0049271 and KEAP1.

HK-2 cells were incubated with Act D (2 μg/ml; Seebio) for 0, 6, 12, 24 h, respectively. At each time point (0, 6, 12, 24 h), RNA was extracted and qRT-PCR was performed for examining the circ_0049271 and KEAP1 expression.

Subcellular fractionation location

The nuclear and cytoplasmic RNA of HK-2 cells was separated using a mirVana PARIS Kit (Invitrogen) followed by

Table 1. Primer sequences used for qRT-PCR

	Primers for PCR (5'-3')		Product size	Accession Number
circ_0049271	F:	GCCAACTTCGCTGAGCAGAT	150	hsa_circ_0049271 (circBase)
	R:	CTGCATGGGGTTCCAGAAGATA		
KEAP1	F:	TGCGTCCTGCACAACTGTAT	199	NM_012289.4 (NCBI)
	R:	CCAGGAACGTGTGACCATCA		
miR-331-3p	F:	CGGCCCCTGGGCCTATC	22	MIMAT0000760 (miRBase)
	R:	AGTGCAGGGTCCGAGGTATT		
GAPDH	F:	GACAGTCAGCCGCATCTTCT	196	NM_002046.7 (NCBI)
	R:	GCGCCCAATACGACCAAATC		
U6	F:	CTCGCTTCGGCAGCACA	96	NR_004394.1 (NCBI)
	R:	AACGCTTCACGAATTTGCGT		

F, forward; R, reverse.

performing qRT-PCR analysis to measure circ_0049271 expression. U6 and GAPDH reprensented the endogenous controls of nucleus and cytoplasm, respectively.

FISH assay

circ_0049271 was labeled by a Cy5 probe (GenePharma, Shanghai, China). According to the instructions of FISH Kit (GenePharma), the signal of circ_0049271 probes was detected in HK-2 cells, and cell nuclei were stained with DAPI. Images were obtained using a confocal microscope.

Cell transfection

The small interfering RNAs of circ_0049271 (si-circ_0049271#1/2), miR-331-3p mimics (miR-331-3p) or inhibitors (anti-miR-331-3p), RUNX1 overexpression plasmid (RUNX1), and their controls were transfected into HK-2 cells *via* Lipofectamine 2000 (Invitrogen). After 24 h, transfected cells were treated with 10 μg/ml LPS for 24 h.

EdU assay

Using the EdU Kit (RiboBio), cells were stained with EdU reagent, fixed with 4% paraformaldehyde, treated with Apollo staining solution, and hatched with DAPI. The percentage of EdU-positive cells was quantified and imaged using a fluorescence microscope (SMZ18, Nikon, Tokyo, Japan).

Oxidative stress assay

The levels of oxidative stress parameters, including SOD, MDA and ROS, were evaluated through SOD Assay Kit, MDA Assay Kit, and ROS Assay Kit (all from Beyotime), respectively.

Cell apoptosis detection

Cells were resuspended with binding buffer and mixed with Annexin V-FITC and PI solution (Sangon, Shanghai, China) for double-staining. A flow cytometer (Agilent, Beijing, China) was utilized to calculate the apoptosis rate.

Western blot

HK-2 cells were incubated with RIPA buffer (Beyotime) for protein extraction. SDS-PAGE was manipulated for protein separation, and proteins were transferred to the PVDF membranes. Membranes were immerged in specific primary antibodies after blocking in 5% skim milk. Subsequently, the second antibody (Goat Anti-Rabbit; 1:5000, ab6721, Abcam, Cambridge, CA, USA) incubation was conducted for 1 h at 37°C. Finally, a ECL reagent kit (Invitrogen) was utilized for protein detection. The primary antibodies used in study including anti-Bcl-2 (26 kD, 1:1000, ab182858), anti-Bax (21 kD, 1:1000, ab32503), anti-c-caspase 3 (17 kD, 1:2000, ab2302), anti-RUNX1 (50 kD, 1:1000, ab240639), and anti-GAPDH (36 kD, 1:2500, ab8245).

ELISA

The culture medium of HK-2 cells was collected for examining the inflammatory cytokines. The IL-1β, IL-8, and TNF-α ELISA detection kits were bought from Beyotime. The detection of IL-1β, IL-8 and TNF-α was conducted referring to the corresponding manual, respectively. The standard curve was drawn, and the corresponding concentration was calculated from the absorbance value of the sample and the standard curve.

Dual-luciferase reporter assay

The circ_0049271-WT/MUT or RUNX1 3'UTR-WT/MUT luciferase plasmids were constructed by cloning wild-type or mutant-type sequences of circ_0049271 or RUNX1 3'UTR containing the miR-331-3p binding sites into pGL3 vectors. The luciferase activity of HK-2 cells co-transfected with the luciferase plasmids and miR-331-3p/miR-NC was measuerd by corresponding kit.

RIP assay

EZ-Magna RIP Kit (Millipore, Billerica, MA, USA) was used to perform RIP assay. After cell lysis, RIP buffer including magnetic beads coated with AGO2 antibody or IgG antibody was mixed with cell lysate for incubation. Finally, RNA was isolated to detect the enrichment of circ_0049271, miR-331-3p, and RUNX1 *via* qRT-PCR.

RNA pull-down assay

HK-2 cells were transfected with bio-miR-331-3p and bio-miR-NC probes (Genepharma). After 48 h of transfection, cell lysates were collected and incubated with Dynabeads M-280 Streptavidin (Invitrogen). Finally, the enrichments of circ_0049271, miR-331-3p and RUNX1 were examined using qRT-PCR.

Statistical analysis

In this research, GraphPad Prism 8.0 software was used for data analysis. Data are exhibited as mean ± SD. All experiments were independently conducted not less than three times. The significant differences among the data were evaluated by Student's *t*-test or ANOVA. $p < 0.05$ was considered statistically significant.

Results

circ_0049271 was up-regulated by LPS-stimulation in HK-2 cells

Given the presence of high expression of circ_0049271 in SAKI patients, we first examined its expression in the LPS-induced HK-2 cell model. The expression of circ_0049271 was dose-dependently increased by LPS stimulation (Fig. 1A). 10 μg/ml LPS was selected to stimulate HK-2 cells for the subsequent experiments. As exhibited in Figure 1B, circ_0049271 is located on chr19:10610070-10610756 and generated by the exon2 of KEAP1. To confirm the cyclic structure, we designed the divergent primers and convergent primers for amplification of circ_0049271 and GAPDH, respectively. Compared to GAPDH, circ_0049271 could only be amplified by divergent primers in cDNA but not in gDNA (Fig. 1C). circ_0049271 was resistant to RNase R treatment, while KEAP1 mRNA was digested by RNase R (Fig. 1D). Moreover, the half-life of circ_0049271 exceeded 24 h and was more stable than KEAP1 mRNA (Fig. 1E). Through subcellular localization analysis and FISH assay, we determined that circ_0049271 was mainly localized in the cytoplasm of HK-2 cells (Fig. 1F,G).

Silencing of circ_0049271 alleviated LPS-induced HK-2 cell injury

As LPS stimulation could induce the expression of circ_0049271, we silenced the circ_0049271 in septic AKI cell model. As shown in Figure 2A, circ_0049271 expression was significantly decreased by transfection of si-circ_0049271#1 and si-circ_0049271#2. Since the si-circ_0049271#1 was more effective for circ_0049271 silencing, it was selectively used in the following experiments. circ_0049271 silencing enahnced EdU positive cell rate in LPS-induced HK-2 cells (Fig, 2B). LPS decreased SOD level and elevated MDA and ROS levels, which could be reversed by transfection with si-circ_0049271#1 (Fig. 2C–E). Then, cell apoptosis rate was strikingly increased after LPS stimulation, while the silenc-

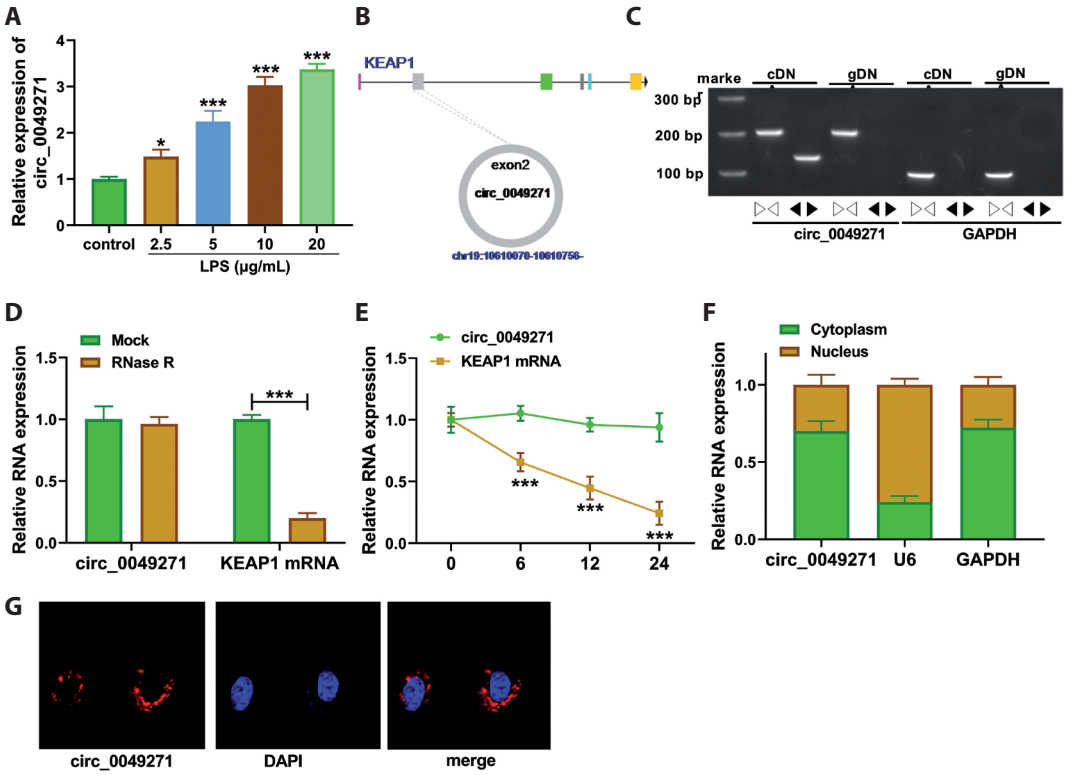

Figure 1. circ_0049271 was increased in LPS-stimulated HK-2 cells. **A.** qRT-PCR detected circ_0049271 expression in HK-2 cells treated with 0, 2.5, 5, 10, 20 μg/ml LPS. **B.** The schematic diagram of circ_0049271 structure. **C.** The PCR pruducts of amplification with divergent primers and convergent primers were shown in agarose gel electrophoresis images. **D.** qRT-PCR examined the enrichment of circ_0049271 and KEAP1 mRNA in HK-2 cell RNA treated with RNase R. **E.** qRT-PCR detected the expression of circ_0049271 and KEAP1 mRNA in HK-2 cells after treatment with Act D. **F.** qRT-PCR was performed to detect the nuclear and cytoplastic expression of circ_0049271. **G.** FISH assay was used to assess the location of circ_0049271 in HK-2 cells. A, E and F: one-way ANOVA followed by Tukey's *post hoc* test; D: two-way ANOVA followed by Tukey's *post hoc* test. * $p < 0.05$, *** $p < 0.001$.

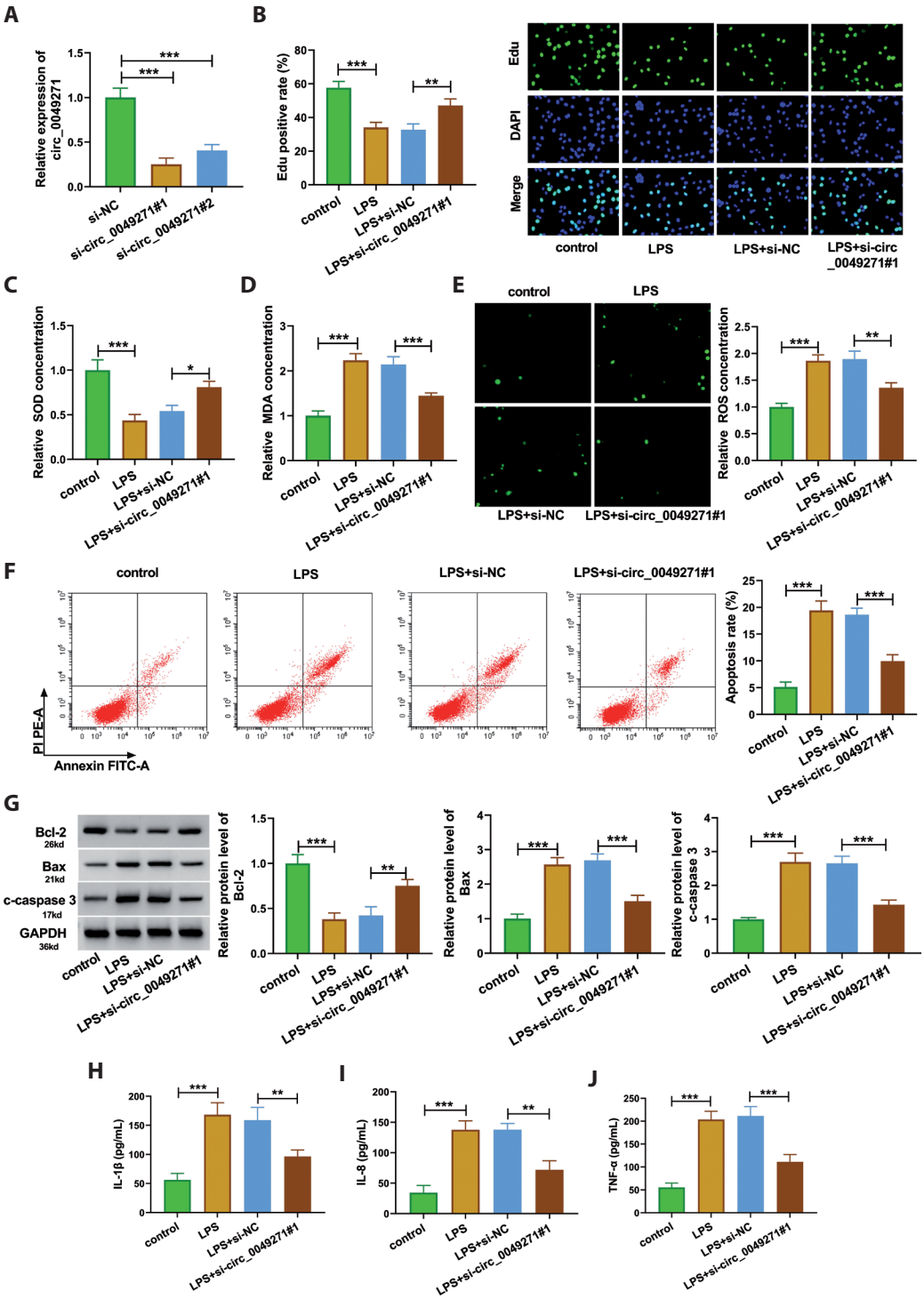

Figure 2. circ_0049271 modulated oxidative stress, apoptosis, and inflammation in LPS-induced HK-2 cells. **A.** The expression of circ_0049271 was detected by qRT-PCR in HK-2 cells transfected with si-NC, si-circ_0049271#1 or circ_0049271#2, respectively. **B.** EdU positive cell rate was examined by EdU assay. The oxidative stress parameters SOD (**C**), MDA, (**D**) and ROS (**E**) were detected by corresponding kits. **F.** Flow cytometry analyzed the cell apoptosis rate. **G.** Western blot assay assessed the levels of apoptosis-related proteins including Bcl-2, Bax, and c-caspase 3. ELISA evaluated the secretion of IL-1β (**H**), IL-8 (**I**), and TNF-α (**J**). B–J: HK-2 cells were transfected with si-NC or si-circ_0049271#1 and treated with 10 μg/ml LPS; A–J: one-way ANOVA followed by Tukey's *post hoc* test. * $p < 0.05$, ** $p < 0.01$, *** $p < 0.001$.

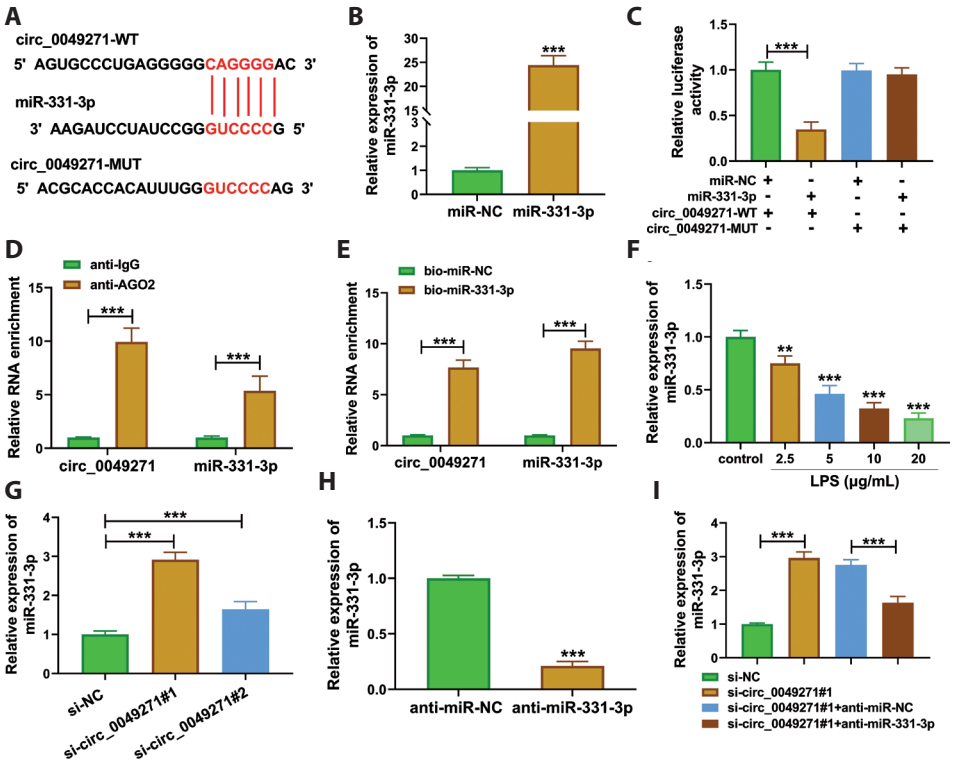

Figure 3. circ_0049271 targeted miR-331-3p in HK-2 cells. **A.** The binding sites between circ_0049271 and miR-331-3p are exhibited. **B.** qRT-PCR detected miR-331-3p expression in HK-2 cells transfected miR-NC or miR-331-3p mimic. Dual-luciferase reporter assay (**C**), RIP assay (**D**), and RNA pull-down assay (**E**) were conducted to verify the binding of circ_0049271 and miR-331-3p. **F.** qRT-PCR measured miR-331-3p expression in HK-2 cells treated with 0, 2.5, 5, 10, 20 μg/ml LPS. **G.** qRT-PCR assessed the miR-331-3p expression in HK-2 cells transfected with si-NC, si-circ_0049271#1, or circ_0049271#2, respectively. **H.** qRT-PCR detected miR-331-3p expression in HK-2 cells transfected with anti-miR-NC or anti-miR-331-3p. **I.** qRT-PCR calculated miR-331-3p expression in HK-2 cells transfected with si-NC, si-circ_0049271#1, si-circ_0049271#1+anti-miR-NC, or si-circ_0049271#1+anti-miR-331-3p, respectively. B and H: Student's *t*-test; C, F, G and I: one-way ANOVA followed by Tukey's *post hoc* test; D and E: two-way ANOVA followed by Tukey's *post hoc* test. ** $p < 0.01$, *** $p < 0.001$.

ing of circ_0049271 relieved this effect (Fig. 2F). As shown in Figure 2G, Bcl-2 protein level was decreased, while the Bax and c-caspase 3 levels were increased in LPS-treated HK-2 cells, but these effects were weakened by silencing circ_0049271. What's more, LPS induced the secretion of IL-1β, IL-8, and TNF-α , while these effects were receded by si-circ_0049271#1 transfection (Fig. 2H–J).

miR-331-3p was a target of circ_0049271 in HK-2 cells

Circinteractome was used to predict the potential targeted miRNAs of circ_0049271. As exhibited in Figure 3A, circ_0049271 had binding sites with miR-331-3p. miR-331-3p expression was greatly enhanced after miR-331-3p mimic transfection (Fig. 3B). The luciferase activity was decreased in cells co-transfected with miR-331-3p and circ_0049271-WT, while it was not affected in other groups (Fig. 3C). Meanwhile, circ_0049271 and miR-331-3p were enriched in AGO2 protein complexes than IgG control group (Fig. 3D). Also, the enrichments of circ_0049271 and miR-331-3p were significantly enhanced by bio-miR-331-3p probe (Fig. 3E). Next, miR-331-3p level was decreased by LPS in a dose-dependent manner (Fig. 3F). Also, miR-331-3p level was remarkably elevated by transfection of si-circ_0049271#1 and si-circ_0049271#2 (Fig. 3G). Moreover, miR-331-3p expression was reduced by anti-miR-331-3p transfection (Fig. 3H). The miR-331-3p expression was enhanced by circ_0049271 silencing, which was reversed by anti-miR-331-3p (Fig. 3I).

circ_0049271 sponged miR-331-3p to regulate LPS-induced HK-2 cell injury

To detect whether the regulation of circ_0049271 on oxidative stress, apoptosis, and inflammation in LPS-induced HK-2 cells was dependent on miR-331-3p, LPS-induced HK-2 cells were co-transfected with anti-miR-331-3p and

si-circ_0049271#1. As shown in Figure 4A, the enhanced EdU positive cell rate caused by si-circ_0049271#1 was attenuated by anti-miR-331-3p in LPS-induced HK-2 cells. Moreover, si-circ_0049271#1 elevated SOD production and decreased MDA and ROS production in LPS-stimulated HK-2 cells, which could be mitigated

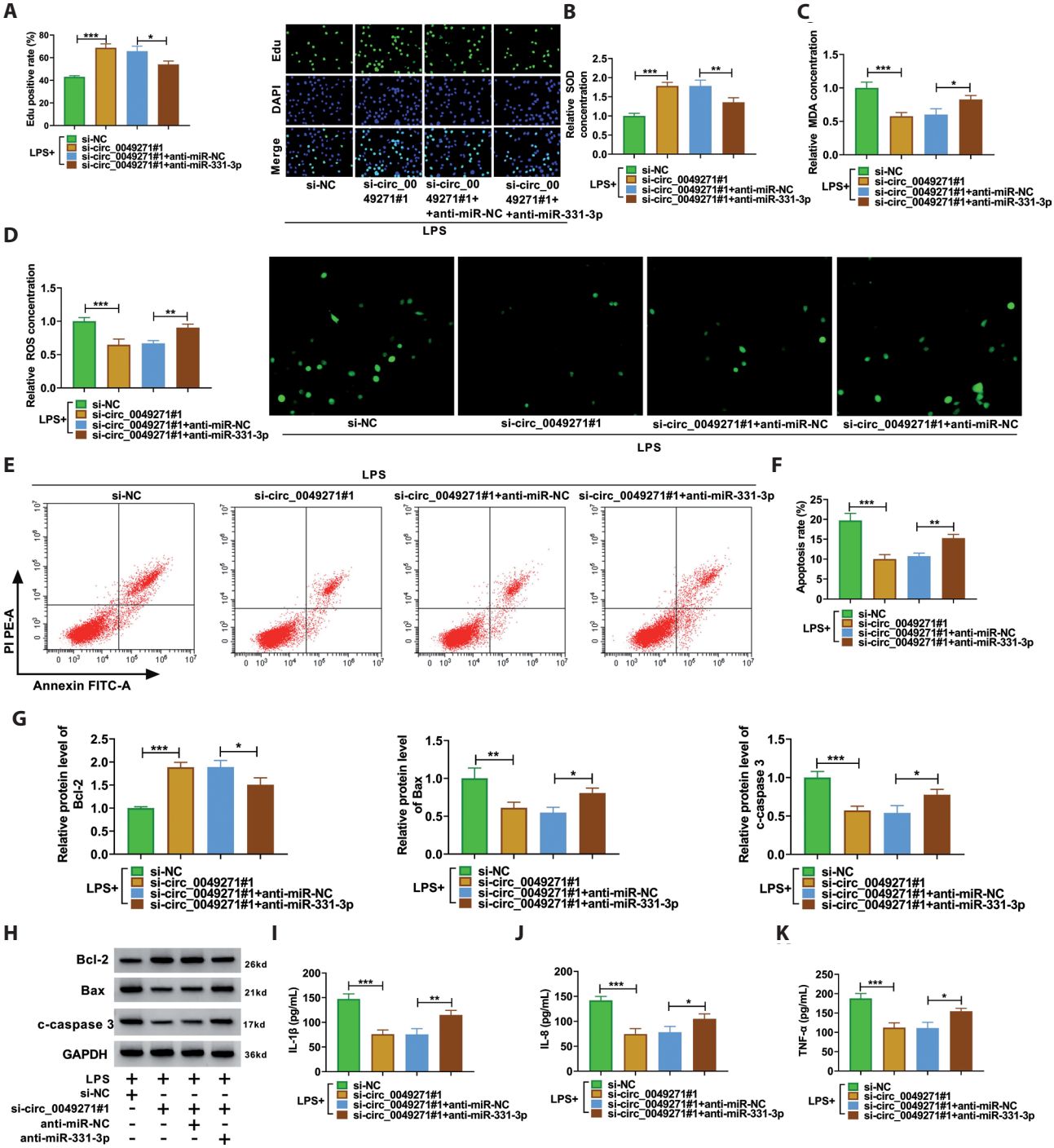

Figure 4. circ_0049271 regulated cell cell oxidative stress, apoptosis, and inflammation in LPS-induced HK-2 cells *via* regulating miR-331-3p. HK-2 cells were transfected with si-NC, si-circ_0049271#1, si-circ_0049271#1+anti-miR-NC, or si-circ_0049271#1+miR-331-3p, and treated with 10 μg/ml LPS. **A.** EdU assay. SOD (**B**), MDA (**C**) and ROS (**D**) were assessed by corresponding kits. **E, F.** Flow cytometry analyzed the cell apoptosis rate. **G, H.** Western blot assay measured the levels of Bcl-2, Bax and c-caspase 3. ELISA evaluated the IL-1β (**I**), IL-8 (**J**) and TNF-α (**K**) secretion by corresponding kits. A–K: one-way ANOVA followed by Tukey's *post hoc* test. * $p < 0.05$, ** $p < 0.01$, *** $p < 0.001$.

with anti-miR-331-3p (Fig. 4B–D). In addition, anti-miR-331-3p was able to abrogate si-circ_0049271#1-mediated inhibiton of cell apoptosis (Fig. 4E,F). Also, silencing of circ_0049271 promoted Bcl-2 expression and inhibited Bax and c-caspase 3 expression, while these effects could be overturned after inhibiting of miR-331-3p (Fig. 4G,H). What's more, the inhibitory effects of circ_004927131 knockdown on IL-1β, IL-8, and TNF-α secretion were abated by anti-miR-331-3p (Fig. 4I–K).

RUNX1 was a target of miR-331-3p in HK-2 cells

Starbase precdicted miR-331-3p could bind with RUNX1, and the binding sites were displayed in Figure 5A. The luciferase activity was notablely decreased in HK-2 cells co-transfected with miR-331-3p and RUNX1 3'UTR but was not changed in other groups (Fig. 5B). Furthermore, the enrichments of RUNX1 and miR-331-3p were increased by anti-AGO2 (Fig. 5C), and RUNX1 and miR-331-3p could be pull-downed by bio-miR-331-3p probe (Fig. 5D). RUNX1 protein level was dose-dependently increased by LPS stimulation (Fig. 5E). Also, over-expression of miR-331-3p could decrease RUNX1 protein level, while miR-331-3p inhibition increased RUNX1 protein level (Fig. 5F). Knockdown of circ_0049271 decreased RUNX1 protein level, which was reversed by anti-miR-331-3p (Fig. 5G). The protein level of RUNX1 was significantly elevated by RUNX1 over-expression (Fig. 5H). In addition, over-expression RUNX1

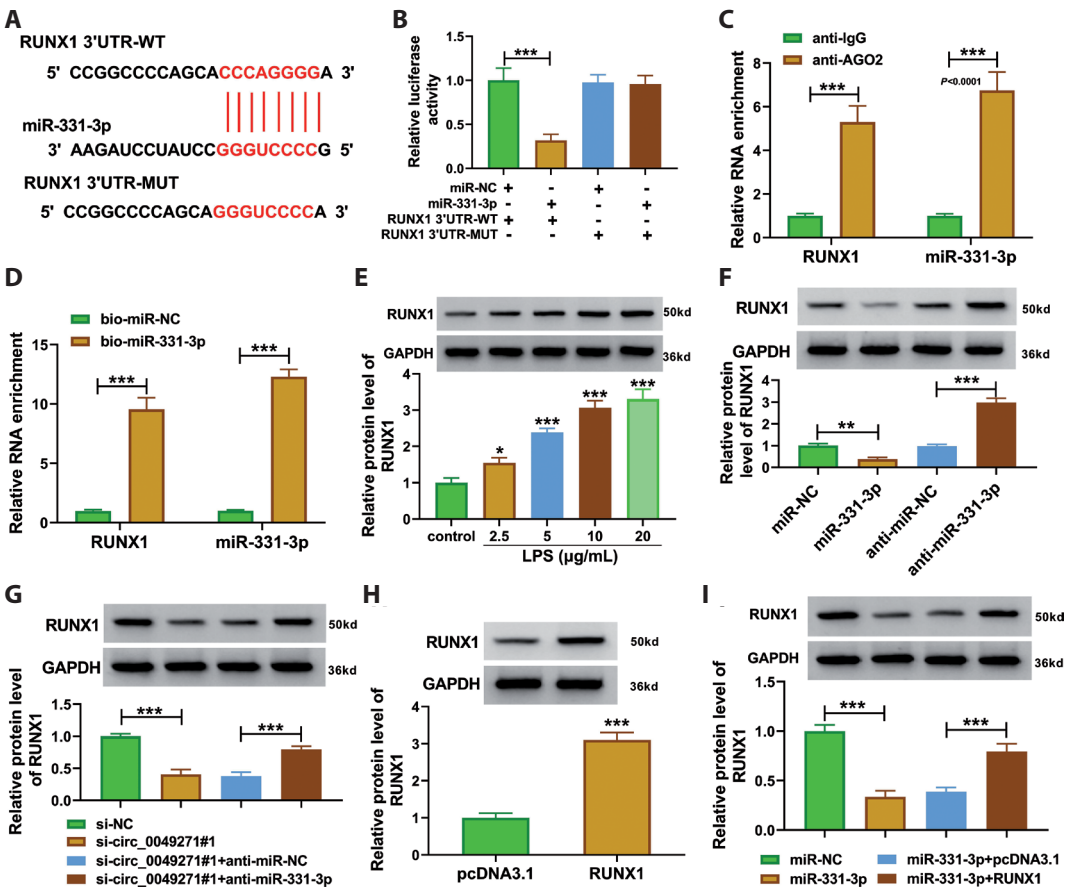

Figure 5. RUNX1 was a target of miR-331-3p in HK-2 cells. **A.** The potential binding sites between miR-331-3p and RUNX1 3'UTR were exhibited. Dual-luciferase reporter assay (**B**), RIP assay (**C**), and RNA pull-down assay (**D**) were performed to verify the binding of miR-331-3p and RUNX1 3'UTR. **E.** Western blot measured RUNX1 protein level in HK-2 cells treated with 0, 2.5, 5, 10, 20 μg/ml LPS. **F.** Western blot tested the RUNX1 protein levels in HK-2 cells transfected with miR-NC, miR-331-3p, anti-miR-NC, or anti-miR-331-3p, respectively. **G.** RUNX1 protein levels in HK-2 cells respectively transfected with si-NC, si-circ_0049271#1, si-circ_0049271#1+anti-miR-NC, or si-circ_0049271#1+anti-miR-331-3p were detected by Western blot. **H.** Western blot detected RUNX1 protein level in HK-2 cells transfected with pcDNA3.1 or RUNX1. **I.** The protein levels of RUNX1 were examined in HK-2 cells severally transfected with miR-NC, miR-331-3p, miR-331-3p+pcDNA3.1, or miR-331-3p+RUNX1 by Western blot. B, E–G and I: one-way ANOVA followed by Tukey's *post hoc* test; C and D: two-way ANOVA followed by Tukey's *post hoc* test; H: Student's *t*-test. * $p < 0.05$, ** $p < 0.01$, *** $p < 0.001$.

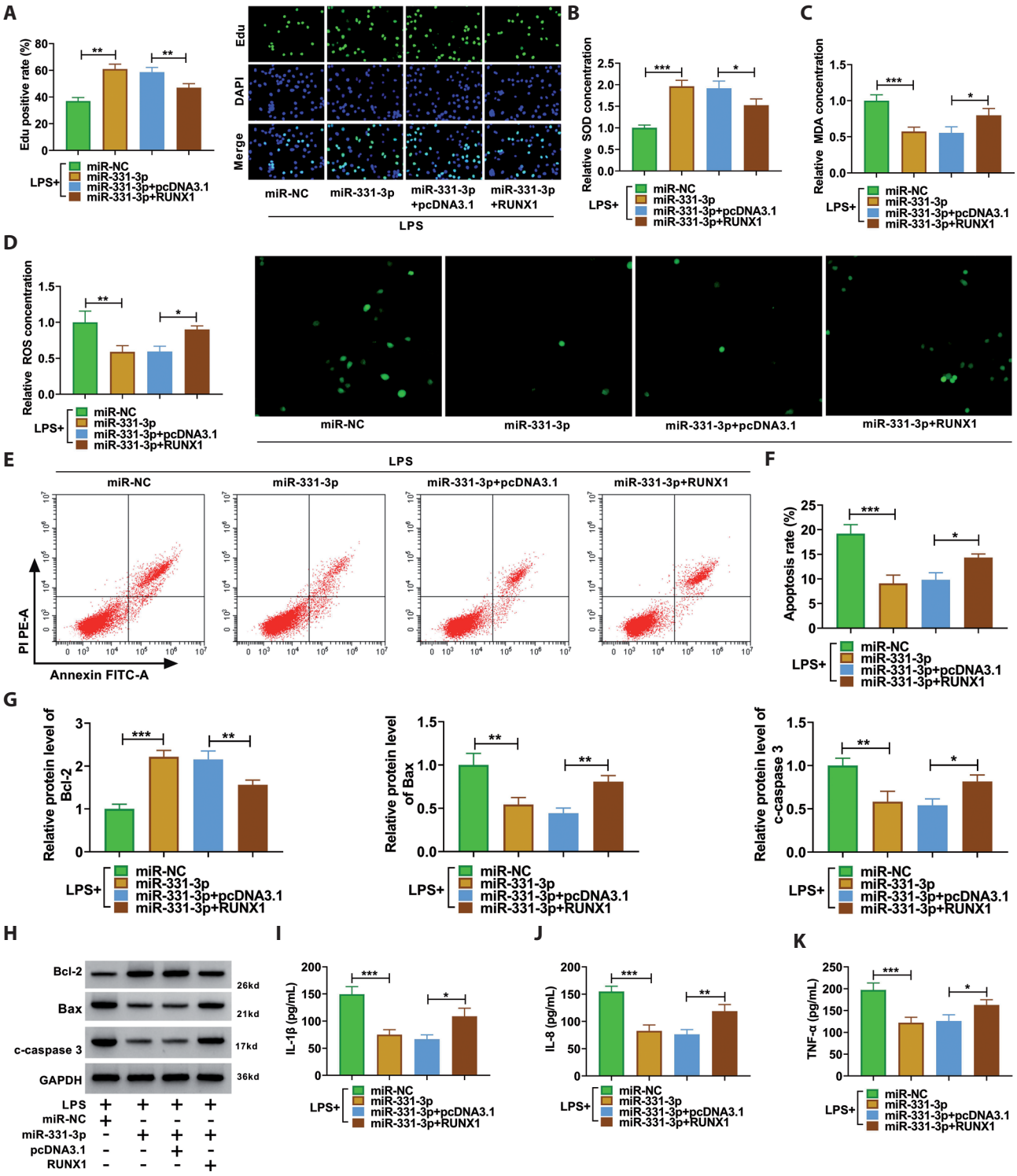

Figure 6. miR-331-3p targeted RUNX1 to regulate cell oxidative stress, apoptosis and inflammation in LPS-induced HK-2 cells. HK-2 cells were transfected with miR-NC, miR-331-3p, miR-331-3p+pcDNA3.1, or miR-331-3p+RUNX1, and treated with 10 μg/ml LPS, respectively. **A.** EdU assay. SOD (**B**), MDA (**C**) and ROS (**D**) were examined by corresponding kits, respectively. **E, F.** Flow cytometry analyzed the cell apoptosis rate. **G, H.** Western blot assay measured the levels of Bcl-2, Bax, and c-caspase 3. ELISA detected the IL-1β (**I**), IL-8 (**J**) and TNF-α (**K**) secretion by corresponding kits, respectively. A–K, one-way ANOVA followed by Tukey's *post hoc* test. * $p < 0.05$, ** $p < 0.01$, *** $p < 0.001$.

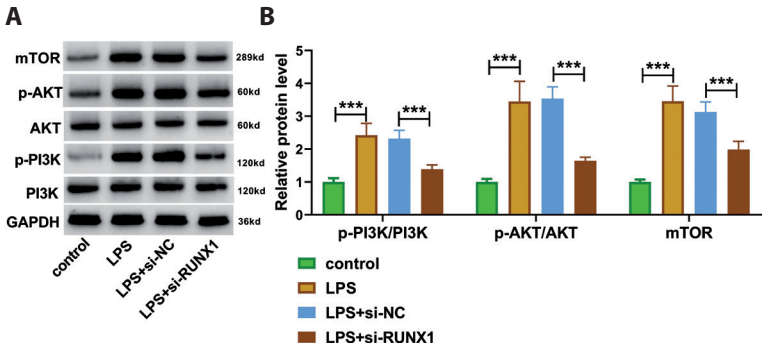

Figure 7. RUNX1 regulated PI3K/AKT/mTOR pathway in LPS-induced HK-2 cells. **A, B.** The protein levels of p-PI3K, PI3K, p-AKT, AKT, and mTOR were examined by Western blot in LPS-induced HK-2 cells transfected with si-NC or si-RUNX1. B: two-way ANOVA followed by Tukey's *post hoc* test. *** $p < 0.001$.

could recede the inhibitory effect of miR-331-3p mimic on RUNX1 expression in HK-2 cells (Fig. 5I).

miR-331-3p attenuated LPS-induced HK-2 cell injury via regulating RUNX1

To validate whether the function of miR-331-3p in LPS-induced HK-2 relies on RUNX1, cells were transfected with miR-331-3p and RUNX1. The miR-331-3p-mediated the enhancement of EdU positive cell rate was mitigated by RUNX1 co-transfection (Fig. 6A). Moreover, the increased SOD and decreased MDA and ROS induced by miR-331-3p were weakened by RUNX1 over-expression (Fig. 6B–D). Furthermore, the inhibitory effect of miR-331-3p on cell apoptosis was overturned by RUNX1 (Fig. 6E,F). Meanwhile, Bcl-2 protein level was increased but the Bax and c-caspase 3 protein levels were decreased by miR-331-3p, and all these effects were reversed by RUNX1 overexpression (Fig. 6G,H). RUNX1 over-expression could abate the inhibitory effects of miR-331-3p on IL-1β, IL-8, and TNF-α secretion (Fig. 6I–K). The PI3K/AKT/mTOR pathway has been found to be activated in SAKI process (Zhao et al. 2020). Here, we showed that LPS treatment could promote the protein levels of p-PI3K, p-AKT, and mTOR, while RUNX1 knockdown significantly inhibited these levels (Fig. 7A,B). To sum up, ous data showed that circ_0049271 sponged miR-331-3p to regulate RUNX1 expression and PI3K/AKT/mTOR pathway, thus affecting LPS-induced HK-2 cell oxidative stress, apoptosis and inflammation (Fig. 8).

Discussion

LPS-induced HK-2 cells has been known as the cell model for investigating SAKI *in vitro* (Wang et al. 2020; Sun et al. 2021). Many previous studies indicate that LPS treatment induces HK-2 cell injury, which is involved in cell apoptosis, inflammation response, oxidative stress, autophagy, pyroptosis, and other biological processes (Li W et al. 2021; Li X et al. 2021; Sun et al. 2021). Moreover, dysregulation of circRNAs induced by LPS can modulate various biological behaviors in SAKI (Wei et al. 2021; Zhou et al. 2021). For example, circVMA21 could attenuate cell apoptosis and inflammation *via* regulating miR-9-3p/SMG1 in LPS-induced

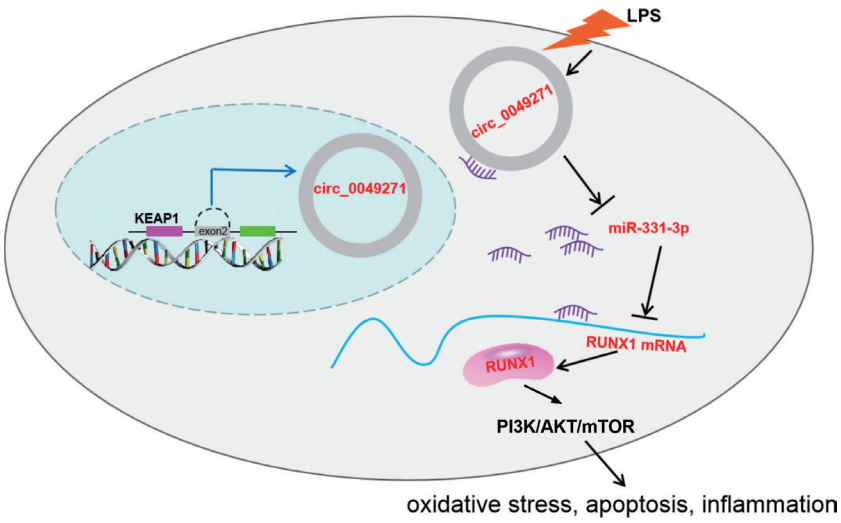

Figure 8. Schematic diagram depicting the action mechanism of circ_0049271 in SKAI. circ_0049271 promotes oxidative stress, apoptosis, and inflammation in LPS-induced HK-2 cells by sponging miR-331-3p to upregulate RUNX1 and activating PI3K/AKT/mTOR pathway.

HK-2 cells (Shi et al. 2020). Previous data of circRNA microarray in serum exosomes of sepsis patients and healthy people showed that circ_0049271 was up-regulated in sepsis serum exosomes (Tian C et al. 2021). However, the role of circ_0049271 in sepsis progression has not been studied. In this study, we demonstrated that circ_0049271 expression was markedly increased in LPS-induced sepsis cell models, which was consistent with the previous research (Tian C et al. 2021). Besides, circ_0049271 silencing suppressed LPS-triggered HK-2 cell oxidative stress, apoptosis, and inflammation response, confirming that targeted inhibition of circ_0049271 might be an effective measure for the treatment of SAKI.

Many abnormally expressed miRNAs are thought to be involved in regulating SAKI progression. For instance, miR-199b-3p was overexpressed in LPS-induced HK-2 cell model, and its inhibition could improve septic AKI *via* Nrf2 pathway (Tian X et al. 2021). For another instance, miR-132-3p was underexpressed in the septic mice relative to the normal mice, and over-expression of miR-132-3p could alleviate kidney injury and inhibit renal cell apoptosis and inflammation response in septic mice through HAVCR1/KIM-1 (Zhang D et al. 2021). By using the bioinformatics website circinteractome, we predicted that miR-331-3p was targeted by circ_0049271. Previous research suggested that miR-331-3p inhibited CLDN2 expression to modulate human vascular endothelial cell injury (Kong et al. 2020). Our study demonstrated that miR-331-3p expression was decreased in LPS-induced sepsis cell models, which was agreeable with the previous study (Kong et al. 2020). Besides, we found that miR-331-3p inhibited LPS-induced HK-2 cell oxidative stress, apoptosis, and inflammation, confirmimg the anti-SAKI role of miR-331-3p. Also, miR-331-3p inhibitor eliminated the inhibition effect of circ_0049271 silencing on LPS-induced cell injury, suggesting that circ_0049271 targeted miR-331-3p to promote SAKI process.

miRNAs can regulate gene transcription through binding with the 3'UTR regions of targeted mRNAs (Tafrihi and Hasheminasab 2019). In our research, we predicted and verified that miR-331-3p could bind to RUNX1 3'UTR. It has been reported that RUNX1 plays a positive role in sepsis process (Luo et al. 2016; Zhang Y et al. 2021). Consistent with this result, our data found that RUNX1 over-expression could reverse the effects of miR-331-3p on cell oxidative stress, apoptosis, and inflammation response, which confirmed the promoting effect of RUNX1 on SAKI process and verified that miR-331-3p targeted RUNX1 to regulate SAKI progression. Moreover, we suggested that the PI3K/AKT/mTOR might be a downstream signal pathway of the circ_0049271/miR-331-3p/RUNX1 axis. Of course, it is necessary to explore whether the circ_0049271/miR-331-3p/RUNX1 axis regulates the PI3K/AKT/mTOR pathway to mediate SAKI process in the future to further enrich our findings.

Of course, there are some limitations of this study. Due to the lack of clinical samples, we only examined circ_0049271, miR-331-3p, and RUNX1 expression in the LPS-induced SAKI cell model. In the future, we still need to collect clinical samples to further confirm the expression trend of circ_0049271, miR-331-3p, and RUNX1 in SAKI patients. Furthermore, we have only studied at the cellular level and have not yet involved *in vivo* experiments. Further animal experiments are necessary and may provide more evidence that the circ_0049271/miR-331-3p/RUNX1 axis regulates SAKI progression.

Conclusion

Taken together, this research illustrated that knockdown of circ_0049271 alleviated LPS-induced HK-2 cell oxidative stress, apoptosis, and inflammation *via* miR-331-3p/RUNX1 axis. Our study is the first to propose the conclusion that the circ_0049271/miR-331-3p/RUNX1 axis regulates LPS-induced kidney cell injury, which provides a new molecular target for SAKI treatment. The proposed circ_0049271/miR-331-3p/RUNX1 axis may provide new ideas for developing the targeted therapeutic targets of clinical SAKI.

Data availability statement. The data used to support the findings of this study are available from the corresponding author upon request.

Conflict of interest. The authors report no declarations of interest.

References

An S, Yao Y, Hu H, Wu J, Li J, Li L, Wu J, Sun M, Deng Z, Zhang Y, et al. (2023): PDHA1 hyperacetylation-mediated lactate overproduction promotes sepsis-induced acute kidney injury via Fis1 lactylation. Cell Death Dis. **14,** 457 https://doi.org/10.1038/s41419-023-05952-4

Beltran-Garcia J, Osca-Verdegal R, Nacher-Sendra E, Pallardo FV, Garcia-Gimenez JL (2020): Circular RNAs in sepsis: Biogenesis, function, and clinical significance. Cells **9,** 1544 https://doi.org/10.3390/cells9061544

Fleischmann-Struzek C, Mellhammar L, Rose N, Cassini A, Rudd KE, Schlattmann P, Allegranzi B, Reinhart K (2020): Incidence and mortality of hospital- and ICU-treated sepsis: results from an updated and expanded systematic review and meta-analysis. Intensive Care Med. **46,** 1552-1562 https://doi.org/10.1007/s00134-020-06151-x

Font MD, Thyagarajan B, Khanna AK (2020): Sepsis and septic shock – Basics of diagnosis, pathophysiology and clinical decision making. Med. Clin. North Am. **104,** 573-585 https://doi.org/10.1016/j.mcna.2020.02.011

Gebert LFR, MacRae IJ (2019): Regulation of microRNA function in animals. Nat. Rev. Mol. Cell. Biol. **20,** 21-37

https://doi.org/10.1038/s41580-018-0045-7
Kim JY, Leem J, Hong HL (2021): Melittin ameliorates endotoxin-induced acute kidney injury by inhibiting inflammation, oxidative stress, and cell death in mice. Oxid. Med. Cell Longev. **2021,** 8843051
https://doi.org/10.1155/2021/8843051
Kong L, Wu P, Li J (2020): miR-331 inhibits CLDN2 expression and may alleviate the vascular endothelial injury induced by sepsis. Exp. Ther. Med. **20,** 1343-1352
https://doi.org/10.3892/etm.2020.8854
Kristensen LS, Andersen MS, Stagsted LVW, Ebbesen KK, Hansen TB, Kjems J (2019): The biogenesis, biology and characterization of circular RNAs. Nat. Rev. Genet. **20,** 675-691
https://doi.org/10.1038/s41576-019-0158-7
Li W, Tan Y, Gao F, Xiang M (2021): Overexpression of TRIM3 protects against LPS-induced acute kidney injury via repressing IRF3 pathway and NLRP3 inflammasome. Int. Urol. Nephrol. **54,** 1331-1342
https://doi.org/10.1007/s11255-021-03017-z
Li X, Yao L, Zeng X, Hu B, Zhang X, Wang J, Zhu R, Yu Q (2021): miR-30c-5p alleviated pyroptosis during sepsis-induced acute kidney injury via targeting TXNIP. Inflammation **44,** 217-228
https://doi.org/10.1007/s10753-020-01323-9
Li X, Tian X, Zhang D (2023): KDM2B regulates inflammation and oxidative stress of sepsis via targeting NF-kappaB and AP-1 pathways. Immun. Inflamm. Dis. **11,** e985
https://doi.org/10.1002/iid3.985
Luo MC, Zhou SY, Feng DY, Xiao J, Li WY, Xu CD, Wang HY, Zhou T (2016): Runt-related transcription factor 1 (RUNX1) binds to p50 in macrophages and enhances TLR4-triggered inflammation and septic shock. J. Biol. Chem. **291,** 22011-22020
https://doi.org/10.1074/jbc.M116.715953
Ma J, Li YT, Zhang SX, Fu SZ, Ye XZ (2019): MiR-590-3p attenuates acute kidney injury by inhibiting tumor necrosis factor receptor-associated factor 6 in septic mice. Inflammation **42,** 637-649
https://doi.org/10.1007/s10753-018-0921-5
Ma P, Zhang C, Huo P, Li Y, Yang H (2020): A novel role of the miR-152-3p/ERRFI1/STAT3 pathway modulates the apoptosis and inflammatory response after acute kidney injury. J. Biochem. Mol. Toxicol. **34,** e22540
https://doi.org/10.1002/jbt.22540
Ma X, Zhu G, Jiao T, Shao F (2021): Effects of circular RNA Ttc3/miR-148a/Rcan2 axis on inflammation and oxidative stress in rats with acute kidney injury induced by sepsis. Life Sci. **272,** 119233
https://doi.org/10.1016/j.lfs.2021.119233
Manrique-Caballero CL, Del Rio-Pertuz G, Gomez H (2021): Sepsis-associated acute kidney injury. Crit. Care Clin. **37,** 279-301
https://doi.org/10.1016/j.ccc.2020.11.010
Nedeva C (2021): Inflammation and cell death of the innate and adaptive immune system during sepsis. Biomolecules **11,** 1011
https://doi.org/10.3390/biom11071011
Poston JT, Koyner JL (2019): Sepsis associated acute kidney injury. BMJ **364,** k4891
https://doi.org/10.1136/bmj.k4891
Qi L, Yan Y, Chen B, Cao J, Liang G, Xu P, Wang Y, Ren Y, Mao G, Huang Z, et al. (2021): Research progress of circRNA as a biomarker of sepsis: a narrative review. Ann. Transl. Med. **9,** 720
https://doi.org/10.21037/atm-21-1247
Shi Y, Sun CF, Ge WH, Du YP, Hu NB (2020): Circular RNA VMA21 ameliorates sepsis-associated acute kidney injury by regulating miR-9-3p/SMG1/inflammation axis and oxidative stress. J. Cell. Mol. Med. **24,** 11397-11408
https://doi.org/10.1111/jcmm.15741
Stasi A, Franzin R, Divella C, Sallustio F, Curci C, Picerno A, Pontrelli P, Staffieri F, Lacitignola L, Crovace A, et al. (2021): PMMA-based continuous hemofiltration modulated complement activation and renal dysfunction in LPS-induced acute kidney injury. Front. Immunol. **12,** 605212
https://doi.org/10.3389/fimmu.2021.605212
Sun M, Li J, Mao L, Wu J, Deng Z, He M, An S, Zeng Z, Huang Q, Chen Z (2021): p53 deacetylation alleviates sepsis-induced acute kidney injury by promoting autophagy. Front. Immunol. **12,** 685523
https://doi.org/10.3389/fimmu.2021.685523
Tafrihi M, Hasheminasab E (2019): MiRNAs: Biology, biogenesis, their web-based tools, and databases. Microrna **8,** 4-27
https://doi.org/10.2174/2211536607666180827111633
Tian C, Liu J, Di X, Cong S, Zhao M, Wang K (2021): Exosomal hsa_circRNA_104484 and hsa_circRNA_104670 may serve as potential novel biomarkers and therapeutic targets for sepsis. Sci. Rep. **11,** 14141
https://doi.org/10.1038/s41598-021-93246-0
Tian X, Liu Y, Wang H, Zhang J, Xie L, Huo Y, Ma W, Li H, Chen X, Shi P (2021): The role of miR-199b-3p in regulating Nrf2 pathway by dihydromyricetin to alleviate septic acute kidney injury. Free Radic. Res. **55,** 842-852
https://doi.org/10.1080/10715762.2021.1962008
Verduci L, Tarcitano E, Strano S, Yarden Y, Blandino G (2021): CircRNAs: role in human diseases and potential use as biomarkers. Cell Death Dis. **12,** 468
https://doi.org/10.1038/s41419-021-03743-3
Wang Z, Wu J, Hu Z, Luo C, Wang P, Zhang Y, Li H (2020): Dexmedetomidine alleviates lipopolysaccharide-induced acute kidney injury by inhibiting p75NTR-mediated oxidative stress and apoptosis. Oxid. Med. Cell Longev. **2020,** 5454210
https://doi.org/10.1155/2020/5454210
Wei W, Yao Y, Bi H, Xu W, Gao Y (2021): Circular RNA circ_0068,888 protects against lipopolysaccharide-induced HK-2 cell injury via sponging microRNA-21-5p. Biochem. Biophys. Res. Commun. **540,** 1-7
https://doi.org/10.1016/j.bbrc.2020.12.018
Xu HP, Ma XY, Yang C (2021): Circular RNA TLK1 promotes sepsis-associated acute kidney injury by regulating inflammation and oxidative stress through miR-106a-5p/HMGB1 axis. Front. Mol. Biosci. **8,** 660269
https://doi.org/10.3389/fmolb.2021.660269
Yang N, Yan N, Bai Z, Du S, Zhang J, Zhang L, Zhang Z (2024): FTO attenuates LPS-induced acute kidney injury by inhibiting autophagy via regulating SNHG14/miR-373-3p/ATG7 axis. Int. Immunopharmacol. **128,** 111483
https://doi.org/10.1016/j.intimp.2023.111483

Zhang D, Lu H, Hou W, Bai Y, Wu X (2021): Effect of miR-132-3p on sepsis-induced acute kidney injury in mice via regulating HAVCR1/KIM-1. Am. J. Transl. Res. **13,** 7794-7803

Zhang Y, Huang H, Liu W, Liu S, Wang XY, Diao ZL, Zhang AH, Guo W, Han X, Dong X, et al. (2021): Endothelial progenitor cells-derived exosomal microRNA-21-5p alleviates sepsis-induced acute kidney injury by inhibiting RUNX1 expression. Cell Death Dis. **12,** 335
https://doi.org/10.1038/s41419-021-03578-y

Zhang Y, Zeng Y, Huang M, Cao G, Lin L, Wang X, Cheng Q (2024): Andrographolide attenuates sepsis-induced acute kidney injury by inhibiting ferroptosis through the Nrf2/FSP1 pathway. Free Radic. Res. **58,** 156-169
https://doi.org/10.1080/10715762.2024.2330413

Zhao Y, Feng X, Li B, Sha J, Wang C, Yang T, Cui H, Fan H (2020): Dexmedetomidine protects against lipopolysaccharide-induced acute kidney injury by enhancing autophagy through inhibition of the PI3K/AKT/mTOR pathway. Front. Pharmacol. **11,** 128
https://doi.org/10.3389/fphar.2020.00128

Zhou Y, Qing M, Xu M (2021): Circ-BNIP3L knockdown alleviates LPS-induced renal tubular epithelial cell injury during sepsis-associated acute kidney injury by miR-370-3p/MYD88 axis. J. Bioenerg. Biomembr. **53,** 665-677
https://doi.org/10.1007/s10863-021-09925-0

Received: January 9, 2025
Final version accepted: April 24, 2025